Available online at www.sciencedirect.com
SCIENCE DIRECT®
Carbohydrate Research 340 (2005) 1818–1825
Carbohydrate RESEARCH

NMR characterization of endogenously O-acetylated oligosaccharides isolated from tomato (*Lycopersicon esculentum*) xyloglucan

Zhonghua Jia, Michael Cash, Alan G. Darvill and William S. York*

Complex Carbohydrate Research Center and Department of Biochemistry and Molecular Biology, University of Georgia, 315 Riverbend Road, Athens, GA 30602-4712, USA

Received 9 March 2005; accepted 24 April 2005
Available online 31 May 2005

Abstract—Eight oligosaccharide subunits, generated by endoglucanase treatment of the plant polysaccharide xyloglucan isolated from the culture filtrate of suspension-cultured tomato (*Lycopersicon esculentum*) cells, were structurally characterized by NMR spectroscopy. These oligosaccharides, which contain up to three endogenous *O*-acetyl substituents, consist of a cellotetraose core with α-D-Xyl*p* residues at O-6 of the two β-D-Glc*p* residues at the non-reducing end of the core. Some of the α-D-Xyl*p* residues themselves bear either an α-L-Ara*p* or a β-D-Gal*p* residue at O-2. *O*-Acetyl substituents are located at O-6 of the unbranched (internal) β-D-Glc*p* residue, O-6 of the terminal β-D-Gal*p* residue, and/or at O-5 of the terminal α-L-Ara*p* residue. Structural assignments were facilitated by long-range scalar coupling interactions observed in the high-resolution gCOSY spectra of the oligosaccharides. The presence of five-bond scalar coupling constants in the gCOSY spectra provides a direct method of assigning O-acetylation sites, which may prove generally useful in the analysis of O-acylated glycans. Spectral assignment of these endogenously O-acetylated oligosaccharides makes it possible to deduce correlations between their structural features and the chemical shifts of diagnostic resonances in their NMR spectra.

Keywords: Xyloglucan; NMR spectroscopy; Structure; Scalar coupling; *Lycopersicon esculentum*; Tomato

1. Introduction

Xyloglucans (XyGs) are major components of primary cell walls, which surround growing plant cells.[1] These water-soluble hemicellulosic polysaccharides spontaneously bind to cellulose microfibrils,[2] forming a load-bearing network that controls the rate and orientation of cell expansion.[3,4] The physical properties that enable XyGs to fulfill this key role in cell-wall growth and development are derived from their chemical structure.[1] XyGs are related to cellulose, with a backbone consisting of β-(1→4)-linked D-Glc*p* residues. In contrast to cellulose, XyGs are highly branched, with up to 75% of the backbone residues bearing a side chain at O-6. The glycosidic linkages of unbranched β-D-Glc*p* residues in the XyG backbone are susceptible to hydrolysis by various endoglucanases (EGs), and EG-treatment of a XyG generates a collection of subunit oligosaccharides, which are small enough to be completely characterized by spectroscopic methods.[5,6]

The identity and distribution of side chains along the XyG backbone is conveniently represented by a sequence of uppercase letters, each of which represent an individual β-D-Glc*p* backbone residue and its pendant side chains.[7] Accordingly, branched β-D-Glc*p* residues bearing an α-D-Xyl*p* side chain, a β-D-Gal*p*-(1→2)-α-D-Xyl*p* side chain, or an α-L-Fuc*p*-(1→2)-β-D-Gal*p*-(1→2)-α-D-Xyl*p* side chain at O-6 are specified as **X**, **L**, or **F**, respectively. Unbranched residues in the XyG backbone are indicated by the letter **G**. Most plant species produce XyGs that can be represented as a sequence

* Corresponding author. Tel.: +1 706 542 4628; fax: +1 706 542 4412; e-mail: will@ccrc.uga.edu

0008-6215/$ - see front matter © 2005 Published by Elsevier Ltd.
doi:10.1016/j.carres.2005.04.015

of these four letters (**X**, **L**, **F**, and **G**).[1] These XyGs have a distinct, regular branching pattern, in which three of the four β-D-Glc*p* residues in the core of each subunit oligosaccharide bear a side chain at O-6, and are referred to as XXXG-type XyGs.[8] The most abundant oligosaccharide subunits in these XyGs are XXXG, XXLG, XXFG, and XLFG. However, XyGs produced by Solanaceous plants have a different branching pattern, in which only two of the four β-D-Glc*p* residues in each subunit bear a side chain at O-6, and are referred to as XXGG-type XyGs.[6,9] In addition, Solanaceous XyGs contain α-L-Ara*f*-(1→2)-α-D-Xyl*p* side chains, represented by the letter **S**, and do not contain fucosylated side chains.[6,9] The most abundant oligosaccharide subunits of these Solanaceous XyGs are XXGG, XSGG, and LSGG.

O-Acetyl substituents have been found at O-6 β-D-Gal*p* residues in the side chains of XXXG-type XyGs.[10,11] XXGG-type XyGs from Solanaceous plants also have *O*-acetyl substituents, in this case at O-6 of β-D-Gal*p* residues and O-5 of α-L-Ara*f* residues in the side chains and at O-6 of the β-D-Glc*p* residues in the backbone.[9,12] Of the two adjacent β-D-Glc*p* residues in XXGG-type XyGs from Solanaceous plants, only the one closest to the non-reducing end typically bears an *O*-acetyl substituent. That is, the core of a typical subunit is XXGG, where the underlined G represents an unbranched β-D-Glc*p* residue that is O-acetylated at O-6. The presence of an *O*-acetyl substituent at O-6 of a β-D-Glc*p* residue inhibits the EG-catalyzed hydrolysis of the glycosidic bond of that residue.[9] Therefore, EG-treatment of an endogenously O-acetylated XXGG-type XyG produces a regular pattern of hydrolysis, in which the great majority of the oligosaccharide fragments have a cellotetraose core.[6] More complex mixtures are generated when XXGG-type XyGs are treated with EG after extraction from the cell wall with strong alkali, as *O*-acetyl substituents are hydrolyzed under the extraction conditions,[9] exposing both of the two adjacent unbranched β-D-Glc*p* residues to hydrolysis by the enzyme.

Purification and structural assignment of XyG oligosaccharides is facilitated by reduction to the corresponding oligoglycosyl alditols using sodium borohydride.[5] This reaction converts the reducing D-Glc*p* residue, which adopts two interconverting anomeric configurations, to an alditol, which can adopt only one configuration. However, borohydride reduction also removes endogenous *O*-acetyl groups, and information regarding the attachment sites of these labile substituents is lost. Complete structural characterization of reducing, endogenously O-acetylated XyG oligosaccharides is complicated by the requirement to purify them from a complex mixture that includes oligosaccharides having different anomeric configurations and O-acetylation patterns.

This paper describes the purification and complete structural characterization of eight reducing oligosaccharides (containing up to three *O*-acetyl substituents) from the XyG produced by suspension-cultured tomato (*Lycopersicon esculentum*) cells. Assignment of the NMR spectra of these oligosaccharides extends the structural reporter approach that we have previously applied to XyG characterization.[1,5,6,9,13] Additional correlations between the chemical shifts of diagnostic resonances and specific structural features are revealed, making it possible to detect, identify, and quantitate specific structural features in complex mixtures of reducing, endogenously O-acetylated XyG oligosaccharides.

2. Results and discussion

XyG was isolated from the medium of suspension-cultured tomato (*L. esculentum*) cells and treated with a xyloglucan-specific endoglucanase (XEG) to generate a mixture of XyG oligosaccharides, which were separated by reversed-phase HPLC. Eight oligosaccharides (XXGG, XXGG, XSGG, XSGG, LLGG, LSGG, LLGG, and LSGG, where the underlined letters indicate the presence of an *O*-acetyl substituent, as illustrated in Fig. 1) were purified. Due to the presence of

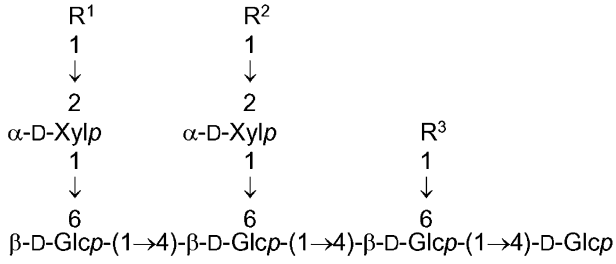

Structure	R^1	R^2	R^3
XXGG	H	H	H
XXGG	H	H	Ac
XSGG	H	α-L-Ara*f*	Ac
XSGG	H	5-*O*-Ac-α-L-Ara*f*	Ac
LSGG	β-D-Gal*p*	5-*O*-Ac-α-L-Ara*f*	Ac
LLGG	β-D-Gal*p*	β-D-Gal*p*	Ac
LLGG	6-*O*-Ac-β-D-Gal*p*	β-D-Gal*p*	Ac
LSGG	6-*O*-Ac-β-D-Gal*p*	5-*O*-Ac-α-L-Ara*f*	Ac

Figure 1. Structures of eight endogenously O-acetylated oligosaccharides prepared from tomato XyG.

O-acetyl substituents and the capacity of each reducing residue to adopt the α- or β-anomeric form, the oligosaccharide mixture was more complex and difficult to separate than the corresponding mixture of oligoglycosyl alditols generated by sodium borohydride reduction.[6] Nevertheless, the purified oligosaccharides were from approximately 75% (LSGG) to 95% homogeneous (LLGG), as judged from the NMR spectra (Fig. 2), allowing their complete structural characterization.

The oligosaccharides were structurally characterized by a combination of MALDI-TOF mass spectrometry and NMR spectroscopy. MALDI-TOF mass spectroscopy provided information regarding the composition of each oligosaccharide, including the number of *O*-acetyl substituents (Table 1). The identity of each glycosyl residue, its linkage to other glycosyl residues, and the presence and location of *O*-acetyl substituents were determined by 2D NMR spectroscopy. The magnetically active nuclei in each glycosyl residue of the oligosaccharides comprise of an isolated spin system that was identified by analysis of crosspeaks that arise in 2D NMR spectra due to homonuclear and heteronuclear scalar coupling interactions.[5,14–17] Measurement of the magnitude of homonuclear ^{1}H:^{1}H scalar couplings provided geometric information that allowed the glycosyl configuration (e.g., β-Glc*p*, α-Xyl*p*, α-Ara*f*, and β-Gal*p*) corresponding to each isolated spin system to be identified.

Table 1. MALDI-TOFMS analysis of native XyG oligosaccharides from tomato cell culture

Measured *m/z*	Composition	Structure
957	Hex_4Pent_2	XXGG
996	Hex_4Pent_2Ac	XXGG[a]
1127	Hex_4Pent_3Ac	XSGG[a]
1169	$Hex_4Pent_2Ac_2$	XSGG[a]
1322	Hex_6Pent_2Ac	LLGG[a]
1332	$Hex_5Pent_3Ac_2$	LSGG[a]
1364	$Hex_6Pent_2Ac_2$	LLGG[a]
1376	$Hex_5Pent_3Ac_3$	LSGG[a]

[a] An underlined letter indicates the presence of an *O*-acetyl substituent. *O*-Acetyl substitution sites were identified by NMR: in G, the acetate is at O-6 of the β-D-Glc*p* residue; in S, the acetate is at O-5 of the α-L-Ara*f* residue; in L, the acetate is at O-6 of the β-D-Gal*p* residue.

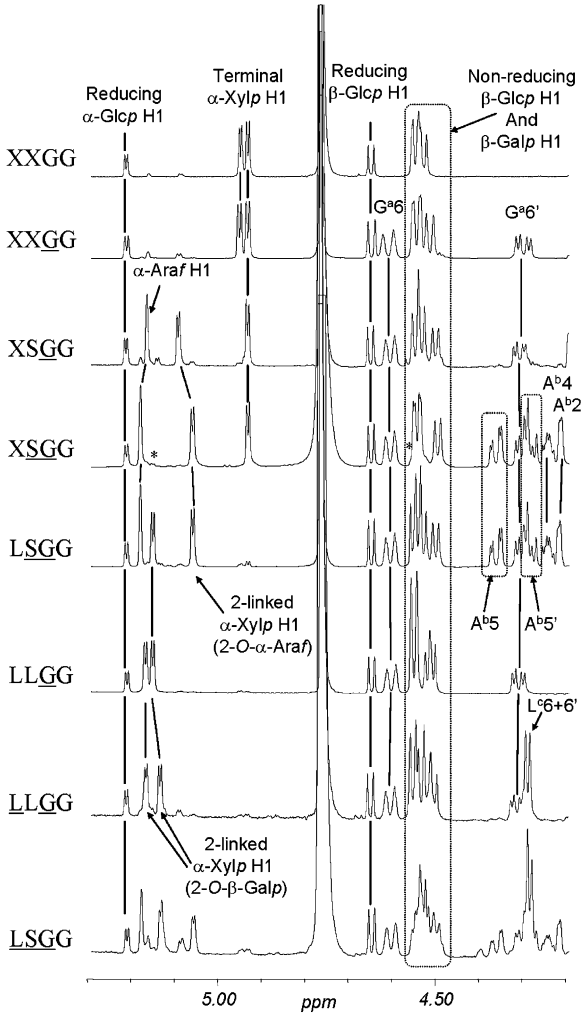

Figure 2. Anomeric region of the ^{1}H NMR spectra of the purified oligosaccharides. Proton resonances shifted into this region by O-acetylation are labeled using an uppercase A, G, or L to indicate a 5-*O*-acetyl α-L-Ara*f*, 6-*O*-acetyl β-D-Glc*p*, or 6-*O*-acetyl β-D-Gal*p* residue, respectively, a superscript lowercase letter (a, b, c) to indicate the location of the residue in the oligosaccharide (see Table 2) and an Arabic number to indicate the proton giving rise to the resonance. For example, G[a]6 indicates one of the methylene protons of a 6-*O*-acetyl β-D-Glc*p* residue that is directly linked to the reducing residue.

Glycosyl linkages between residues were identified by analysis of heteronuclear multiple bond correlation (HMBC) spectra[18] and in high-resolution gradient-selected homonuclear correlation (gCOSY) spectra. For example, heteronuclear $^{3}J_{H1,C4'}$ and $^{3}J_{C1,H4'}$ couplings give rise to crosspeaks in the HMBC spectra of oligosaccharides with (1→4)-linkages (data not shown). We have previously shown[6] that the sequence of β-D-Glc*p* residues in a XyG oligosaccharide backbone can be determined by analysis of interresidue $^{4}J_{H1,H4}$ couplings that are observed[19] in high-resolution gCOSY spectra (boxed crosspeaks in Fig. 3). These long-range homonuclear couplings are relatively weak, giving rise to crosspeaks that have approximately the same intensity as crosspeaks arising from vicinal and geminal couplings in minor oligosaccharide contaminants of the purified samples described here. For example, the 1D ^{1}H NMR spectrum of the XSGG sample contained two weak signals (marked by asterisks in Fig. 2) that suggest the presence of a small amount (~10%) of LSGG as a contaminant. One of these signals (δ 5.159) has a chemical shift diagnostic for H-1 of an α-Xyl*p* residue bearing a β-Gal*p* residue at O-2. The other weak signal (δ 4.559) corresponds to H-1 of the contaminating β-Gal*p* residue itself, and is barely perceptible as a shoulder on a strong anomeric proton signal. The gCOSY spectrum of the

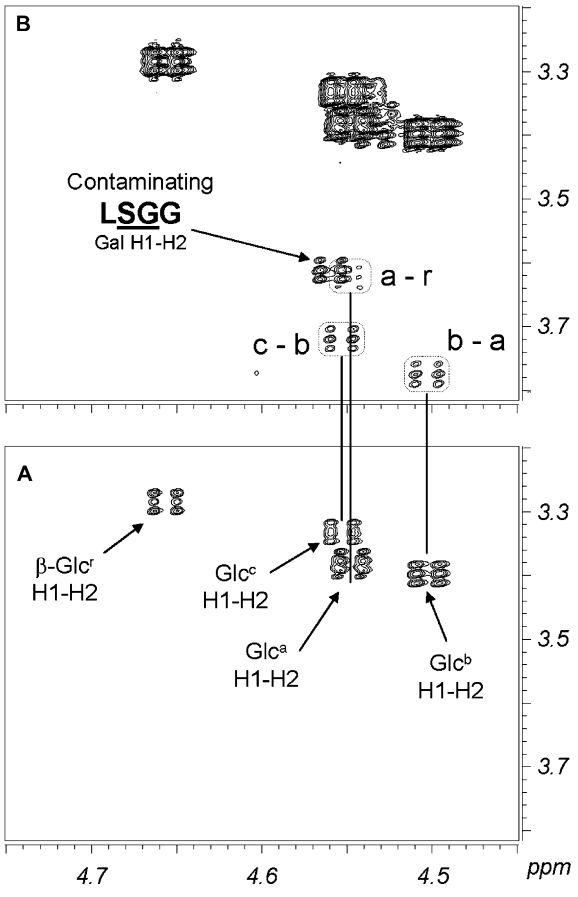

Figure 3. Region of the high-resolution gCOSY spectrum of XSGG containing long-range ($^4J_{H1,H4'}$ scalar couplings that provide backbone sequence information. (A) Spectrum drawn at contour levels that show only crosspeaks due to short-range (geminal and vicinal) scalar coupling for protons in XSGG, the major component (>90%). (B) Spectrum drawn at contour levels that show crosspeaks due to short-range scalar coupling in minor components (e.g., LSGG) and long-range scalar couplings in XSGG. Each interglycosidic crosspeak, surrounded by a dotted line, correlates H-1 of a β-D-Glc*p* to H-4 of its aglycon (another D-Glc*p* residue). The location of the two (1→4)-linked residues correlated by each crosspeak is indicated by the lowercase letters, as described in the footnotes to Table 2. A small amount of contaminating LSGG is present in the sample. Vicinal (H-1–H-2) scalar coupling in the terminal β-D-Gal*p* residue of this contaminant gives rise to a crosspeak that does not vertically align with any of the high intensity crosspeaks (panel A) arising from XSGG, the major component of the sample.

XSGG sample (Fig. 3) contains a crosspeak due to the vicinal $^3J_{H1,H2}$ for this contaminating β-Gal*p* residue. This $^3J_{H1,H2}$ crosspeak is incompletely resolved from an interglycosidic $^4J_{H1,H4}$ crosspeak that is diagnostic for the glycosidic linkage between Glc^a and Glc^r of XSGG, the major component of the sample (see footnotes of Table 2 for nomenclature). The β-Gal*p* $^3J_{H1,H2}$ crosspeak could be assigned to a contaminating species due to the fact that it is not vertically aligned with any of the major H-1 resonances arising from XSGG (Fig. 3).

Somewhat unexpectedly, homonuclear $^5J_{H6,Me}$ and $^5J_{H5,Me}$ couplings, which correlate *O*-acetyl CH_3 protons with the proton attached to the carbon bearing an *O*-acetyl substituent, were also observed in the gCOSY spectra of the tomato XyG oligosaccharides (Fig. 4). Although ^5J couplings have been previously observed,[19] this may be their first application to the site-specific assignment of *O*-acetyl substituents in oligosaccharides. Analysis of these very long-range scalar interactions may prove useful for characterizing other types of acylated oligosaccharides.

2.1. Structure–chemical shift correlations

Several correlations diagnostic for the presence and location of *O*-acetyl substituents on XyG oligosaccharides were revealed (Fig. 2). Although the downfield shift of protons attached to carbons bearing *O*-acetyl substituents has already been well established,[11] analysis of the tomato XyG oligosaccharides allowed H-6 resonances of *O*-acetate-bearing β-D-Gal*p* (side chain), and β-D-Glc*p* (backbone) residues and H-5 resonances of *O*-acetate-bearing α-L-Ara*f* (side-chain) residues to be specifically identified by their characteristic chemical shifts (Fig. 2, Table 2). For example, the geminal H-6 resonances of the 6-*O*-acetyl β-D-Gal*p* residue terminating the side chain attached to the non-reducing end of the backbone of LLGG and LSGG are degenerate, with a diagnostic chemical shift (δ 4.293). This pattern is distinct from that observed for the H-6 resonances of 6-*O*-acetyl β-D-Gal*p* residues of side chains attached to an internal backbone residue.[10] The chemical shifts of protons not directly attached to the *O*-acetate-bearing carbons are also affected by acetylation, but to a lesser extent. For example, the H-1, H-4, H-3, and H-2 resonances of α-L-Ara*f* residues terminating side chains attached to Glc^b are all shifted downfield by O-acetylation at C-5. A similar effect is observed for the ring protons of β-D-Gal*p* residues that terminate side chains at the non-reducing end of the backbone, except that H-1 is shifted upfield by O-acetylation. In general, the chemical shift of H-1 of an α-D-Xyl*p* side-chain residue is shifted upfield when the α-L-Ara*f* or β-D-Gal*p* residue that it bears at O-2 is O-acetylated, consistent with our previous unpublished observations. Finally, the observation of long-range ($^5J_{HH}$) scalar couplings allowed the position of the *O*-acetyl substituents to be correlated to the chemical shifts of their methyl proton resonances. That is, a resonance at δ 2.15 is correlated to the presence of an *O*-acetyl group at C-6 of a β-D-Glc*p* (backbone) residue or C-5 of an α-L-Ara*f* (side-chain) residue, while a resonance at δ 2.12 is correlated to the presence of an *O*-acetyl group at C-6 of a β-D-Gal*p* (side-chain) residue.

Table 2. ^{1}H NMR chemical shift assignments for the oligosaccharides

Residue	H-1	H-2	H-3	H-4	H-5	H-5e	H-6	H-6*
				XXGG				
Xyl^{c}	4.940	3.542	3.731	3.611	3.500	3.709	—	—
Xyl^{b}	4.956	3.542	3.722	3.617	3.591	3.713	—	—
Glc^{c}	4.553	3.338	3.518	3.518	3.696	—	3.777	3.935
Glc^{b}	4.556	3.388	3.671	3.737	3.823	—	3.901	4.005
Glc^{a}	4.535	3.364	3.659	3.674	3.622	—	3.823	3.975
α-Glc^{r}	5.220	3.571	3.818	3.639	3.942	—	3.866	3.866
β-Glc^{r}	4.656	3.277	3.629	3.656	3.592	—	3.803	3.948
				XXGG				
Xyl^{c}	4.940	3.541	3.731	3.604	3.549	3.713	—	—
Xyl^{b}	4.958	3.546	3.726	3.614	3.724	3.580	—	—
Glc^{c}	4.551	3.342	3.520	3.520	3.698	—	3.782	3.937
Glc^{b}	4.521	3.386	3.660	3.726	3.828	—	4.005	3.910
Glc^{a}	4.558	3.377	3.669	3.754	3.847	—	4.305	4.616
α-Glc^{r}	5.219	3.575	3.815	3.691	3.946	—	3.851	3.851
β-Glc^{r}	4.655	3.281	3.625	3.625	3.596	—	3.804	3.947
Ac (Glc^{a})	2.147							
				XSGG				
Ara^{b}	5.171	4.196	3.937	4.081	3.936	3.846	—	—
Xyl^{c}	5.940	3.543	3.731	3.611	3.545	3.710	—	—
Xyl^{b}	5.100	3.574	3.858	3.668	3.734	3.564	—	—
Glc^{c}	4.540	3.331	3.520	3.520	3.687	—	3.744	3.939
Glc^{b}	4.508	3.394	3.657	3.677	3.838	—	3.948	3.948
Glc^{a} (Ac)	4.554	3.384	3.666	3.782	3.847	—	4.311	4.613
α-Glc^{r}	5.220	3.577	3.815	3.612	3.947	—	3.859	3.859
β-Glc^{r}	4.657	3.284	3.619	3.629	3.605	—	3.804	3.945
Ac (Glc^{a})	2.151							
				XSGG				
Ara^{b} (Ac)	5.189	4.222	4.023	4.254	4.371	4.291	—	—
Xyl^{c}	4.940	3.547	3.738	3.613	3.557	3.726	—	—
Xyl^{b}	5.069	3.565	3.854	3.678	3.558	3.738	—	—
Glc^{c}	4.555	3.335	3.519	3.688	3.850	—	3.943	3.781
Glc^{b}	4.504	3.399	3.657	3.718	3.809	—	3.972	3.985
Glc^{a} (Ac)	4.551	3.386	3.671	3.773	3.853	—	4.613	4.311
α-Glc^{r}	5.221	3.581	3.816	3.623	3.950	—	3.868	3.868
β-Glc^{r}	4.658	3.286	3.617	3.623	3.632	—	3.949	3.807
Ac (Glc^{a})	2.149							
Ac (Ara^{b})	2.149							
				LLGG				
Gal^{c}	4.556	3.608	3.649	3.922	n.a.	—	n.a.	n.a.
Gal^{b}	4.554	3.616	3.649	3.922	n.a.	—	n.a.	n.a.
Xyl^{c}	5.165	3.681	3.914	3.652	3.562	3.717	—	—
Xyl^{b}	5.173	3.673	3.922	3.654	3.582	3.729	—	—
Glc^{c}	4.513	3.342	3.513	3.457	3.735	—	3.813	3.733
Glc^{b}	4.524	3.410	3.662	3.662	3.894	—	3.965	3.921
Glc^{a} (Ac)	4.556	3.388	3.679	3.794	3.850	—	4.311	4.609
α-Glc^{r}	5.215	3.573	3.812	3.620	3.938	—	3.864	3.864
β-Glc^{r}	4.654	3.281	3.617	3.617	3.595	—	3.803	3.944
Ac (Glc^{a})	2.151							
				LSGG				
Gal^{c}	4.559	3.613	3.658	3.922	3.688	—	3.767	3.767
Ara^{b} (Ac)	5.185	4.225	4.022	4.252	4.293	4.371	—	—
Xyl^{c}	5.159	3.686	3.916	3.668	3.562	3.718	—	—
Xyl^{b}	5.066	3.564	3.857	3.673	3.739	3.571	—	—
Glc^{c}	4.537	3.337	3.514	3.453	3.732	—	3.813	3.882
Glc^{b}	4.509	3.409	3.660	3.729	3.814	—	3.922	3.984
Glc^{a} (Ac)	4.549	3.385	3.674	3.774	3.853	—	4.309	4.612
α-Glc^{r}	5.219	3.579	3.814	3.623	3.950	—	3.866	3.866
β-Glc^{r}	4.656	3.286	3.620	3.630	3.596	—	3.805	3.946
Ac (Glc^{a})	2.147							
Ac (Ara^{b})	2.147							

Table 2 (*continued*)

Residue	H-1	H-2	H-3	H-4	H-5	H-5e	H-6	H-6*
				LLGG				
Gal^{c} (Ac)	4.538	3.621	3.664	3.950	3.900	—	4.293	4.293
Gal^{b}	4.557	3.620	3.664	3.922	n.a.	—	n.a.	n.a.
Xyl^{c}	5.140	3.639	3.915	3.568	3.566	3.717	—	—
Xyl^{b}	5.174	3.673	3.921	3.655	3.582	3.729	—	—
Glc^{c}	4.506	3.341	3.506	3.430	3.737	—	3.790	3.875
Glc^{b}	4.525	3.412	3.664	3.664	3.895	—	3.967	3.920
Glc^{a} (Ac)	4.557	3.389	3.681	3.796	3.851	—	4.312	4.608
α-Glc^{r}	5.216	3.573	3.814	3.621	3.938	—	3.866	3.866
β-Glc^{r}	4.655	3.281	3.617	3.617	3.595	—	3.804	3.944
Ac (Glc^{a})	2.152							
Ac (Gal^{c})	2.122							
				LSGG				
Gal^{c}	4.540	3.622	3.655	3.951	3.898	—	4.294	4.294
Ara^{b}	5.187	4.224	4.020	4.251	4.291	4.370	—	—
Xyl^{c}	5.142	3.638	3.919	3.653	3.576	3.717	—	—
Xyl^{b}	5.066	3.562	3.854	3.667	3.731	3.572	—	—
Glc^{c}	4.533	3.335	3.508	3.427	3.730	—	3.791	3.878
Glc^{b}	4.509	3.410	3.655	3.731	3.813	—	3.982	3.926
Glc^{a} (Ac)	4.552	3.384	3.670	3.775	3.848	—	4.612	4.311
α-Glc^{r}	5.219	3.576	3.813	3.622	3.948	—	3.866	3.866
β-Glc^{r}	4.656	3.282	3.621	3.628	3.594	—	3.803	3.945
Ac (Glc^{a})	2.146							
Ac (Ara^{b})	2.146							
Ac (Gal^{c})	2.119							

Superscript a, b, c, and r indicate the location of the residue vis-à-vis the reducing end. That is, the β-D-Glc*p* residues in the backbone are specified as Glc^{c}→Glc^{b}→Glc^{a}→Glc^{r}, where Glc^{r} is the reducing β-D-Glc*p* residue. The locations of side-chain residues are indicated by the superscript letter of the backbone residue to which the side chain is attached. Underlined residues bear an *O*-acetyl substituent at the methylene carbon (C-5 or C-6). n.a. indicates the resonance was not assigned.

2.2. Conclusions

Spectroscopic analysis of eight oligosaccharides prepared from the medium of suspension-cultured tomato (*L. esculentum*) cells established additional correlations between specific structural features and the chemical shifts of diagnostic resonances in the ^{1}H NMR spectra of XyG oligosaccharides. These correlations can be used to rapidly identify structural elements of this class of biologically important glycans, as illustrated by the accompanying paper.[20] The analysis also demonstrates the power of using long-range ($^{4}J_{HH}$ and $^{5}J_{HH}$) scalar coupling (observed in high-resolution gCOSY spectra) as a tool to determine the attachment sites of glycosyl and it *O*-acetyl substituents.

3. Experimental

3.1. Preparation and endoglucanase treatment of XyG

XyG was prepared from the culture medium of suspension-cultured tomato (*L. esculentum* var. 'Bonnie Best') cells. The tomato XyG (6.6 g) was treated as described[6] for 48 h at ambient temperature in 20 mM NaOAc buffer (pH 5) with 100 units of xyloglucan-specific endoglucanase (XEG), generously provided by Novozymes (Copenhagen, Denmark) and purified as previously described.[21] MALDI-TOFMS was used to monitor the generation of oligosaccharides, and when no further change in molecular weight of the products was observed, three volumes of 95% EtOH were added to precipitate other polymers (mainly galactoglucomannan), which were removed by centrifugation (10 min at 3000*g*). The supernatant was concentrated to remove EtOH and desalted on Sephadex G-25. The anthrone assay for hexoses[22] was used to detect XyG oligosaccharides in the eluent, and salt-free fractions were pooled and lyophilized (700 mg).

3.2. Purification of XyG oligosaccharides

The XyG oligosaccharides were partially separated by size-exclusion chromatography on two Bio-Gel P-2 columns (−400 mesh, 96 × 1.6 cm) connected in series, and eluted with deionized water.[5,6] Partially purified oligosaccharides were further separated by reversed-phase HPLC on octadecyl silica (Hibar Lichrosob RP-18, column dimensions 1.0 × 25 cm). A typical chromatographic separation involved the injection of 100–200 μL of a concentrated Bio-Gel P-2 fraction and elution with aq MeOH (6–15% v/v at 2.0 mL/min).

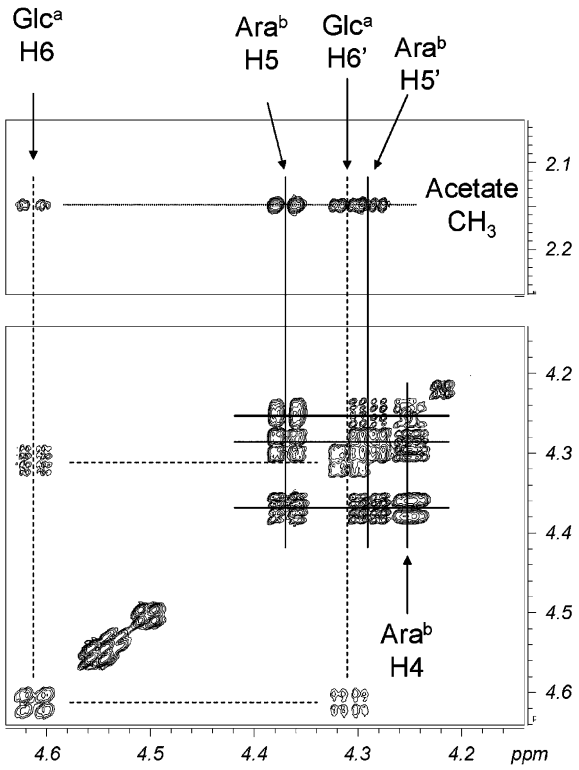

Figure 4. Regions of the gCOSY spectrum of XSGG revealing long-range (^5J) scalar couplings that provide information regarding the location of *O*-acetyl substituents. The bottom panel is drawn using contour levels that show only crosspeaks due to short-range (geminal and vicinal) scalar couplings. The top panel shows a different region of the spectrum drawn using contour levels revealing long-range (^5J) couplings between the methylene protons of the O-acetylated residues and the methyl protons of the O-acetyl substituents. Connectivities for the β-D-Gal*p* residue are indicated with dashed lines and those for the α-L-Ara*f* are indicated with solid lines.

Evaporative light scattering (SEDEX 55 ELSD, S.E.D.E.R.E., Alfortville, France) was used to detect oligosaccharides in the eluent.

3.3. Matrix-assisted laser-induced/ionization time-of-flight mass spectrometry (MALDI-TOFMS)

A Hewlett–Packard LDI 1700 XP spectrometer operating with an accelerating voltage of 30 kV, an extractor voltage of 9 kV, and a source pressure of approximately 8×10^{-7} Torr was used to record the MALDI-TOF mass spectra of the oligosaccharides. Aqueous oligosaccharide solutions were mixed with the ionization matrix consisting of (1:1 v/v) 2,5-dihydroxybenzoic acid (DHB, 0.2 M) and 1-hydroxyisoquinoline (HIC, 0.06 M), both in 50% aq CH_3CN, applied to the MALDI probe, and dried in vacuo.

3.4. Nuclear magnetic resonance (NMR) spectroscopy

Solutions of the purified oligosaccharides (in 600 μL of 99.96% enriched ^2H_2O) were transferred to 5-mm NMR tubes, and spectra were recorded at 298 K with a Varian Inova 600 NMR spectrometer using standard Varian pulse sequences. Two-dimensional NMR spectra[17] (COSY,[19] TOCSY, NOESY, gHSQC, and HMBC) were recorded. Mixing times were 100 and 500 ms for the TOCSY and NOESY, respectively. Typically, 512 FIDs consisting of 1024 data points were recorded with a spectral width of 1500 Hz in both dimensions, and the data were processed using NMR pipe[23] and the Mestrec software.[24] At least 800 FIDs were recorded for high-resolution gCOSY spectra, with zero filling to obtain a 2048×2048 matrix. Chemical shifts were measured relative to internal acetone at δ 2.225.

Acknowledgments

This research was supported in part by funds from the U.S. Department of Energy (DOE) grant DE-FG02-96ER20220 and from the DOE-funded Center for Plant and Microbial Complex Carbohydrates (DE-FG02-93ER20097). The authors would like to thank Novozymes A/S who generously provided the xyloglucan-specific endoglucanase used in this research.

References

1. O'Neill, M. A.; York, W. S. The composition and structures of primary cell walls. In *The Plant Cell Wall*; Rose, J. K. C., Ed.; CRC Press: Boca Raton, FL, 2003; Vol. 8, pp 1–54.
2. Valent, B. S.; Albersheim, P. *Plant Physiol.* **1974**, *54*, 105–108.
3. Whitney, S. E. C.; Brigham, J. E.; Darke, A. H.; Reid, J. S. G.; Gidley, M. J. *Plant J. Cell Mol. Biol.* **1995**, *8*, 491–504.
4. Carpita, N. C.; Gibeaut, D. M. *Plant J.* **1993**, *3*, 1–30.
5. York, W. S.; van Halbeek, H.; Darvill, A. G.; Albersheim, P. *Carbohydr. Res.* **1990**, *200*, 9–31.
6. Jia, Z. H.; Qin, Q.; Darvill, A. G.; York, W. S. *Carbohydr. Res.* **2003**, *338*, 1197–1208.
7. Fry, S. C.; York, W. S.; Albersheim, P.; Darvill, A. G.; Hayashi, T.; Joseleau, J.-P.; Kato, Y.; Lorences, E. P.; Maclachlan, G. A.; McNeil, M.; Mort, A. J.; Reid, J. S. G.; Seitz, H. U.; Selvendran, R. R.; Voragen, A. G. J.; White, A. R. *Physiol. Plant.* **1993**, *89*, 1–3.
8. Vincken, J.-P.; York, W. S.; Beldman, G.; Voragen, A. G. *Plant Physiol.* **1997**, *114*, 9–13.
9. York, W. S.; Kolli, V. S. K.; Orlando, R.; Albersheim, P.; Darvill, A. G. *Carbohydr. Res.* **1996**, *285*, 99–128.
10. York, W. S.; Oates, J. E.; van Halbeek, H.; Darvill, A. G.; Albersheim, P. *Carbohydr. Res.* **1988**, *173*, 113–132.
11. Kiefer, L. L.; York, W. S.; Darvill, A. G.; Albersheim, P. *Phytochemistry* **1989**, *28*, 2105–2107.
12. Sims, I. M.; Munro, S. L.; Currie, G.; Craik, D.; Bacic, A. *Carbohydr. Res.* **1996**, *293*, 147–172.
13. York, W. S.; Impallomeni, G.; Hisamatsu, M.; Albersheim, P.; Darvill, A. G. *Carbohydr. Res.* **1995**, *267*, 79–104.
14. Vliegenthart, J. F. G.; Dorland, L.; van Halbeek, H. *Adv. Carbhydr. Chem. Biochem.* **1983**, *41*, 209–374.

15. Bush, C. A. *Bull. Magn. Reson.* **1988**, *10*, 73–95.
16. Dabrowski, J. Application of Two-Dimensional NMR Methods in the Structural Analysis of Oligosaccharides and Other Complex Carbohydrates. In *Two Dimensional NMR Spectroscopy: Applications for Chemists and Biochemists*; Croasmun, W. R., Carlson, R. M. K., Eds.; VCH: New York, 1987, pp 349–386.
17. Kessler, H.; Gehrke, M.; Griesinger, C. *Angew. Chem., Int. Ed. Engl.* **1988**, *27*, 490–536.
18. Bax, A.; Summers, M. F. *J. Am. Chem. Soc.* **1986**, *108*, 2093–2094.
19. Otter, A.; Bundle, D. R. *J. Magn. Reson. Ser. B* **1995**, *109*, 194–201.
20. Hoffman, M.; Jia, Z.; Pena, M. J.; Cash, M.; Harper, A.; Blackburn, A. J.; Darvill, A. G.; York, W. S. *Carbohydr. Res.* **2005**, *340*, in this issue, please see doi:10.1016/j.carres.2005.04.016.
21. Pauly, M.; Andersen, L. N.; Kauppinen, S.; Kofod, V.; York, W. S.; Albersheim, P.; Darvill, A. G. *Glycobiology* **1999**, *9*, 93–100.
22. Dische, Z. *Methods Carbohydr. Chem.* **1962**, *1*, 478–481.
23. Delaglio, F.; Grzesiek, S.; Vuister, G. W.; Zhu, G.; J., P.; A., B. *J. Biomol. NMR* **1995**, *6*, 277–293.
24. Cobas, J. C.; Sardina, F. J. *Concepts Magn. Reson.* **2003**, *19A*, 80–96.